

**UNCLASSIFIED**

---

**AD 275 055**

*Reproduced  
by the*

**ARMED SERVICES TECHNICAL INFORMATION AGENCY  
ARLINGTON HALL STATION  
ARLINGTON 12, VIRGINIA**



---

**UNCLASSIFIED**

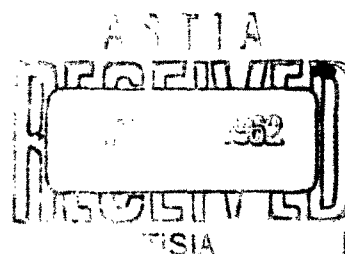
# AFESD - TDR - 62- 81

## Table of Contents

Abstract .....	ii
Introduction .....	1
The Drag Formula .....	2
Finess Ratio .....	6
Weights .....	7
Appendix I .....	9
Appendix II .....	12
List of Symbols .....	18
References .....	19
Distribution List .....	20

## List of Figures

Figure 1, Blunted Cone-Sphere Configuration .....	14
Figure 2, Graphs of $C_D$ vs $\eta$ .....	15
Figure 3, Graphs of $W/R_b^2$ vs $\eta$ .....	16
Figure 4, Graphs of Finess Ratio vs $\eta$ .....	17



### ABSTRACT

A simple formula for the Newtonian drag coefficient is derived for the blunted cone-sphere ("ice-cream cone") at small angles of attack. Graphs are presented for  $C_D$  as a function of cone semi-vertex angle from  $6^\circ$  to  $30^\circ$  and "bluntness ratio" (nose-radius/base-radius) ranging in tenths from 0 to 0.5. For given values of the body parameters, the weight required for the body to attain a prescribed ballistic coefficient is then determined. Fineness ratios for different specified cone-angles and degrees of bluntness are provided for reference.

Introduction. Newtonian impact theory makes two basic assumptions: first, that the shock wave lies along the body-surface; second, that in striking the body, the airstream loses the component of momentum normal to the surface -- the flow is regarded as continuing along the surface with the tangential component of momentum unchanged.

The local pressure coefficient obtained under the Newtonian hypothesis therefore depends only on the local inclination of the surface to the airstream:

$$C_p = 2 \left( \frac{v_n}{v_\infty} \right)^2$$

where  $v_\infty$  and  $v_n$  are the free-stream velocity and its component normal to the body-surface respectively. \*  $C_p$  is taken to be zero over those portions of the surface shielded from the flow.

The second of the basic assumptions made above neglects centrifugal forces associated with curvature of the body surface, and the condition of the first assumption is attained only in the limit as  $M_\infty \rightarrow \infty, \gamma \rightarrow 0$ . ( $M_\infty$  is the free-stream Mach number and  $\gamma$  the ratio of specific heats.) In this connection, the relevant parameter appears not to be the Mach number itself so much as the ratio  $M_\infty/F$ , where  $F$  is the body fineness ratio

$$F = \text{Total body-length/Maximum body-diameter.}$$

---

\* See Appendix I.

For values of  $M_\infty/F$  less than 2 for example, Newtonian estimates of the local pressure coefficient for cones have been found<sup>2</sup> to be in error by more than 17%. On the other hand, Newtonian theory has been found to give qualitative and even quantitative information of acceptable accuracy in practical cases of interest at hypersonic speeds, and the following computations of drag coefficients and related quantities should prove useful even at high altitudes when the contributions of viscous effects \* and ablation are incorporated.

The following sections are concerned with a single configuration at small angles of attack. The body studied consists of a cone-frustum capped at both ends by tangent spherical surfaces. Cone semi-vertex angles between  $6^\circ$  and  $30^\circ$  are considered with bluntness ratios (nose-radius/base-radius) ranging in tenths from 0 to 0.5. Under the assumption of negligible pitching and zero angle of attack, a simple formula is derived for the corresponding Newtonian drag coefficients. This was programmed for the IBM 7090, and the tabulated values of  $C_D$  so generated have been presented in graphical form. Also presented are estimates (based on  $C_D$ ) of the weight required for the body to have a prescribed ballistic coefficient. Fineness ratios are given for reference.

The Drag Formula. The blunted cone-sphere configuration to be considered has rotational symmetry. A coordinate system will be chosen with origin at the nose and  $x$  measured along the axis of symmetry. (See Figure 1.) With the surface then described by the radial distance  $R = R(x)$ , the axial-force coefficient  $C_X$  may be found by integration over the surface actually exposed to the flow:

---

\* These are relatively important for sharp-nosed bodies during early re-entry.

$$C_X = \frac{1}{A} \iint C_p \sin \theta \, dS$$

where  $A$  is the reference-area and  $\theta = \arctan R'(x)$ . \*

If the angle of attack is small, so that the entire surface between the planes  $x = 0$  and  $x = l$  is that exposed to the flow, and if furthermore the angular pitch-rate  $q$  is negligible in comparison with the velocity  $v_\infty$ , then integration and simplification \*\* lead to an approximate expression for the drag coefficient:

$$C_D = C_X = \frac{4\pi}{A} \int_0^l \frac{R(x) R'(x)^3}{1 + R'(x)^2} \, dx \quad (0)$$

where the interval  $[0, l]$  is to be broken into three segments corresponding to the different definitions of  $R$  over the nose, midsection, and base of the body.

A spherical tip of radius  $R_n$  is generated by revolving a segment of the circle  $[x - R_n]^2 + [R(x)]^2 = R_n^2$ ; the radial distance for the nose portion of the body is therefore

$$R = [2R_n x - x^2]^{1/2} \quad \text{for } 0 \leq x \leq x_1, \quad (1)$$

---

\* See Appendix I.

\*\* See Appendix II.

where tangency occurs at  $x_1$ . We denote by  $\eta$  the (constant) semi-vertex angle of the conical midsection, and note that

$$x_1 = R_n - R_n \sin \eta$$

The radial distance for the midsection is then simply

$$R = [x + x_1 / \sin \eta] \tan \eta \quad \text{for } x_1 \leq x \leq x_2, \quad (2)$$

where the spherical back, having radius  $R_b$ , is tangent at

$$x_2 = \ell - R_b \sin \eta.$$

Finally, the portion of the spherical back which is not shielded from the airstream has radial distance

$$R = [R_b^2 - (x - \ell)^2]^{1/2} \quad \text{for } x_2 \leq x \leq \ell, \quad (3)$$

where the maximum radius of the body is  $R_b = R(\ell)$

Computation of  $C_D$  as represented by equation (0) thus requires the integration of three separate expressions,  $R$  being defined in the respective intervals as noted above:

$$\frac{R R'^3}{1 + R'^2} = \begin{cases} (R_n - x)^3 / R_n^2 & \text{for } 0 \leq x \leq x_1, \\ R R' \sin^2 \eta & \text{for } x_1 \leq x \leq x_2, \\ (\ell - x)^3 / R_b^2 & \text{for } x_2 \leq x \leq \ell. \end{cases} \quad (4)$$

The second expression is easily handled with  $R$  as independent variable going between  $R_n \cos \eta$  and  $R_b \cos \eta$ , and the other two integrations are routine.

We shall find it convenient now to take as reference-area the maximum cross-section of the body,

$$A = \pi R_b^2.$$

Substitution and integration of (4) in equation (0) then yields

$$C_D = \kappa^2 (1 - \sin^4 \eta) + 2(1 - \kappa^2) \sin^2 \eta \cos^2 \eta + \sin^4 \eta, \quad (5)$$

where we have introduced the "bluntness ratio"  $\kappa = R_n/R_b$  as a convenient parameter. A trigonometric identity now gives a simple formula for  $C_D$  as a function of  $\kappa$  and  $\eta$ :

$$C_D = \kappa^2 \cos^4 \eta + [2 - \sin^2 \eta] \sin^2 \eta. \quad (6)$$

The same technique demonstrated above has been used to find  $C_D$  for the case of a blunted cone which has a flat back at distance  $x = \ell$  from the nose. The corresponding formula (obtained on replacing  $x_2$  by  $\ell$  in equation (4)) is offered for comparison:

$$C_D = \kappa^2 \cos^4 \eta + 2 \sin^2 \eta \quad (\text{flat back}).$$



The obvious similarity of the two expressions conforms to the expected similarity of body-shape when  $\eta$  is small. It should be noted that the formula we have derived for the cone with spherical back differs from the flat-back case not only in the presence of a  $(\sin^4 \eta)$ -term whose contribution may be negligibly small if  $\kappa/\eta$  is large; but also, for a given nose-radius, base-radius, and exposed body-length  $\ell$ , the spherical back gives a larger semi-cone angle  $\eta$  than does the flat back.

A final simplification of equation (6) gives a concise formula for the Newtonian drag coefficient of a blunted cone-sphere at small angles of attack:

$$C_D = 1 - [1 - \kappa^2] \cos^4 \eta$$

$$\text{where } \kappa = R_n/R_b \text{ and } A = \pi R_b^2.$$

Fineness Ratio It is easy to verify that the semi-vertex angle  $\eta$  in a blunted cone-sphere satisfies the relation

$$\sin \eta = (R_b - R_n)/(\ell - R_n).$$

If the total body length is denoted by  $L$ , then  $\ell = L - R_b$ , and we may use the fact that the fineness ratio is  $F = L/2R_b$  to write instead

$$\sin \eta = (1 - \kappa)/(2F - [\kappa + 1]),$$

determining the angle  $\eta$  when the ratios of  $R_n$ ,  $R_b$ , and  $L$  are known. The relation between  $\eta$  and  $F$  expressed by this equation is presented graphically for different values of the bluntness ratio  $\kappa$  in Figure 4.

It may be of interest for comparison to note that the semi-vertex angle  $\eta'$  for a flat-backed cone satisfies the relation

$$\sin \eta' = (R_b \cos \eta' - R_n)/(L - R_n),$$

where for this case  $l = L$ . It follows that if a cone with spherical back were to have the same bluntness and fineness ratios, it would have to have a (larger) semi-vertex angle  $\eta$ , determined by the ratio

$$\frac{\sin \eta}{\sin \eta'} = \frac{1 - \kappa}{(\cos \eta' - \sin \eta') - \kappa}$$

Weights. While nearly constant over considerable altitude ranges in the case of blunt-nosed bodies, the ballistic coefficient (or "weight-to-drag" ratio)  $W/C_D A$  may vary appreciably at high altitudes for sharp-nosed bodies. Viscous drag is relatively insignificant at 50,000 feet however, and common usage seems to base  $W/C_D A$  on the (pressure) drag at this altitude when no further qualification is mentioned. Since maximum deceleration of a high performance re-entry body might be expected to occur at an even lower altitude (determined by the ballistic coefficient and the re-entry path angle), the Newtonian value of  $C_D$  may therefore prove useful in estimating the weight required for a specified ballistic coefficient to be attained.

If the desired ballistic coefficient is  $\beta$ , then substituting for the reference-area  $A$  gives

$$W/R_b^2 = \pi C_D \beta.$$

The accompanying graphs of  $W/R_b^2$  vs  $\eta$  for different values of  $\kappa$  are based for scaling convenience on a ballistic coefficient of 100 lbs/ft<sup>2</sup>. Hence, for a given semi-vertex angle  $\eta$  (degrees), bluntness ratio  $\kappa$ , and base-radius  $R_b$ (ft), the weight  $W$  (lbs) necessary for a ballistic coefficient  $\beta$  (lbs/ft<sup>2</sup>) is given by

$$W = [W/R_b^2] \cdot R_b^2 \cdot \frac{\beta}{100} ,$$

where the expression in brackets is the value read off from the appropriate curve.

# APPENDIX I

The component of free-stream velocity  $V_\infty$  which is in the direction of a normal  $\vec{n}$  to the surface-element  $dS$  has magnitude

$$v_n = V_\infty \cos \angle \vec{n},$$

so the mass striking  $dS$  normally in unit time is the product of the volume generated and the free-stream density  $\rho_\infty$ :

$$dm = \rho_\infty (v_n dS).$$

The rate of change of momentum of the mass striking  $dS$  in the direction of the normal gives the local pressure-force

$$dF = (p - p_\infty) dS = v_n dm = \rho_\infty v_n^2 dS,$$

where  $p$  and  $p_\infty$  are the local pressure and the free-stream pressure respectively.

As a function of the local pressure difference  $(p - p_\infty)$  and the free-stream dynamic pressure

$$q_\infty = \frac{1}{2} \rho_\infty V_\infty^2,$$

the local pressure coefficient

$$C_p = \frac{p - p_\infty}{q_\infty} = 2 \left( \frac{v_n}{V_\infty} \right)^2$$

thus depends only on the local inclination of the surface to the airstream. (The flow is considered to be completely separated with  $C_p = 0$  over those portions of the surface shielded from the flow.)

We are concerned with a smooth body having axial symmetry. Its surface, accordingly, may be described by giving the radial distance  $R$  as a differentiable function of just the distance  $x$  measured from the nose of the body (as origin) along the axis of symmetry. The local inclination of the surface with respect to this axis is then

$$\theta = \theta(x) = \arctan R'(x).$$

When there is an angle of attack  $\alpha$ , the local pressure coefficient varies not only with  $x$  but also with the angle  $\omega$  measured in a plane orthogonal to the axis. (See Figure 1.)  $C_p$  is thus dependent on  $\alpha$ ,  $\theta$ , and  $\omega$ . \*

The above relations being understood, the force acting on an area-element  $dS$  may be expressed simply as

$$dF = q_\infty C_p dS.$$

The component of this force in the direction of the axis is then  $(\sin \theta) dF$ , and integrating over the portion of the surface actually exposed to the airstream gives the total axial force

$$F_X = q_\infty \iint C_p \sin \theta dS.$$

---

\* See Appendix II.

The non-dimensional axial-force coefficient  $C_X$ , defined with respect to the reference-area  $A$  by the relation

$$F_X = q_\infty (C_X A),$$

may therefore be represented in the following form:

$$C_X = \frac{1}{A} \iint C_p \sin \theta \, dS.$$

Expressing the element of area  $dS$  by  $(R \, d\omega) (dx/\cos\theta)$  and substituting formally then gives

$$C_X = \frac{1}{A} \int \left( \int C_p R R' \, d\omega \right) dx$$

with integration limits corresponding to the surface exposed to the flow.

## APPENDIX II

The longitudinal axis of symmetry of the body, directed positively back from the nose, has been chosen as the X-axis of the body coordinate system. The free-stream velocity vector is assumed to be at a small angle of attack  $\alpha$  (of no greater magnitude than  $\eta$ ) relative to the X-axis, determining with it a plane in which pitching occurs about the center of gravity  $x_{cg}$  at an angular rate  $q$ .

With these conventions, the local normal component of velocity  $v_n$  may be expressed<sup>1,3</sup> in the form

$$v_n = v_\infty \cos \alpha [ \sin \theta - \tan \alpha \sin \omega \cos \theta ] - q \sin \omega [ (x - x_{cg}) \cos \theta + R \sin \theta ],$$

or equivalently, upon substituting for  $\cos \theta$  and  $\tan \theta$ ,

$$v_n(x, \omega) = \frac{v_\infty \cos \alpha}{\sqrt{1 + R'^2}} \left[ R' - \sin \omega \left( \frac{q}{v_\infty \cos \alpha} [RR' + x - x_{cg}] + \tan \alpha \right) \right].$$

It then follows from definition of  $C_p$  that

$$C_p(x, \alpha, \omega) = \frac{2 \cos^2 \alpha}{1 + R'^2} (R' - G \sin \omega)^2$$

where

$$G(x) = \frac{q}{v_\infty \cos \alpha} [RR' + x - x_{cg}] + \tan \alpha.$$

The entire surface corresponding to  $0 \leq x \leq l$  and  $0 \leq \omega \leq 2\pi$  is exposed to the flow at small angles of attack ( $\alpha < \eta$ ), so the surface integral defining  $C_X$  may be evaluated as an iterated integral with these limits on  $x$  and  $\omega$ . Taking advantage of symmetry, we obtain

$$C_X = \frac{2}{A} \int_0^l \int_{-\pi/2}^{+\pi/2} R(x) R'(x) C_p(x, \alpha, \omega) d\omega dx.$$

It remains to substitute for  $C_p$  in the form obtained above:

$$\int_{-\pi/2}^{+\pi/2} (R' - G \sin \omega)^2 d\omega = (2R'^2 + G^2) \frac{\pi}{2},$$

$$\therefore C_X = \left[ \frac{4\pi}{A} \int_0^l \frac{RR'^3}{1+R'^2} dx \right] \cos^2 \alpha + \frac{2\pi}{A} \int_0^l \frac{RR'}{1+R'^2} (G \cos \alpha)^2 dx.$$

The drag-force is directly opposed to the body's velocity-vector (relative to the flow) at an angle  $\alpha$  from the axis, and the integrand on the right is clearly bounded with  $q$ . Hence the relation  $\cos \alpha \sim 1$  for small  $\alpha$  and the assumption that  $(q/v_\infty)^2$  is negligible leaves just the bracketted expression asserted in equation (0).



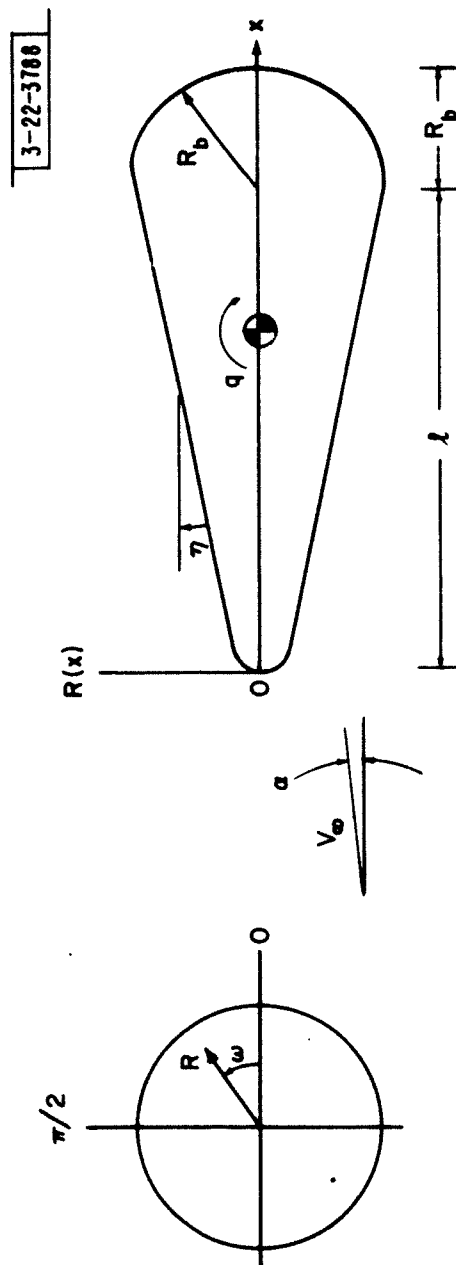


Fig. 1. Blunted cone-sphere.

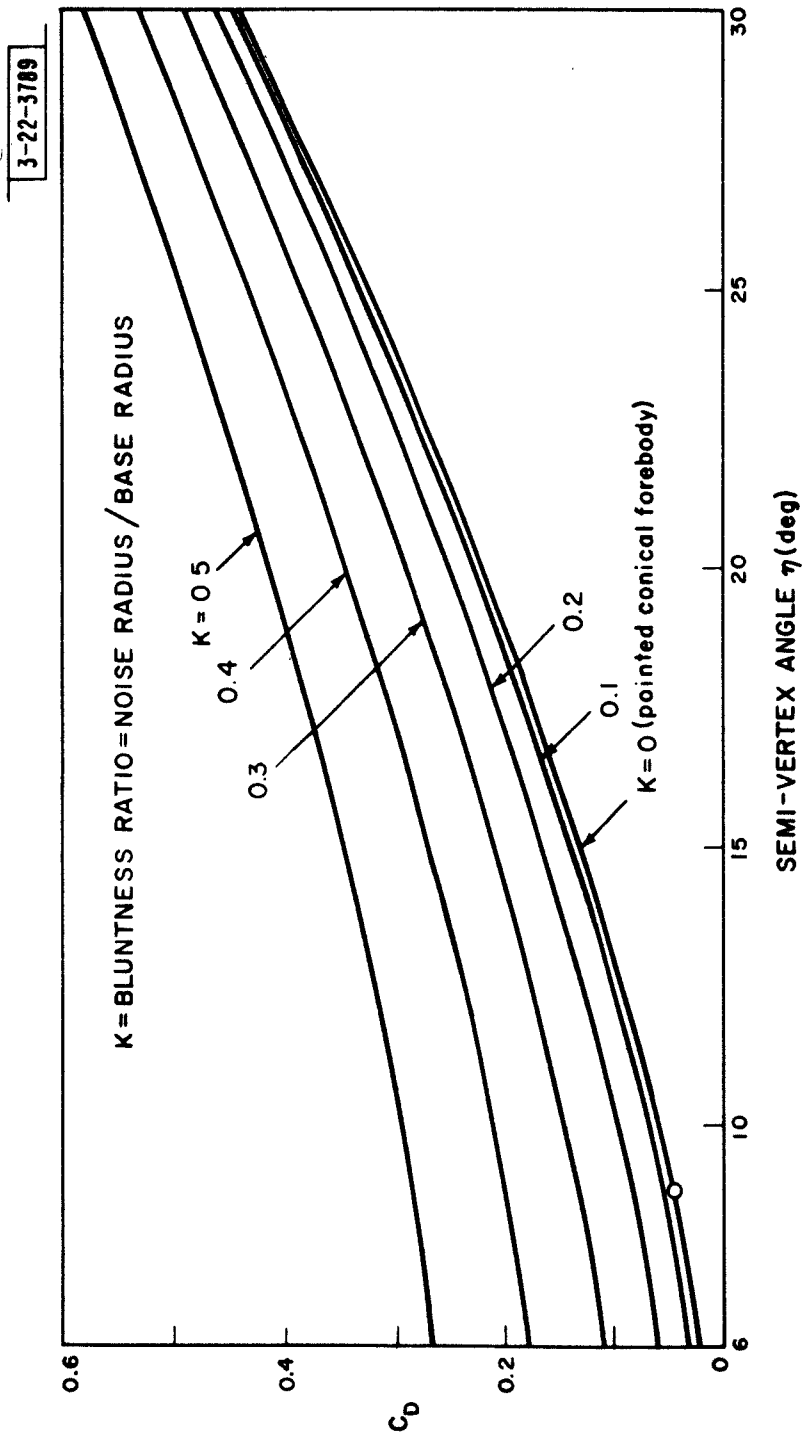


Fig. 2. Newtonian drag coefficients for blunted cone-spheres ( $\alpha = 0$ ).

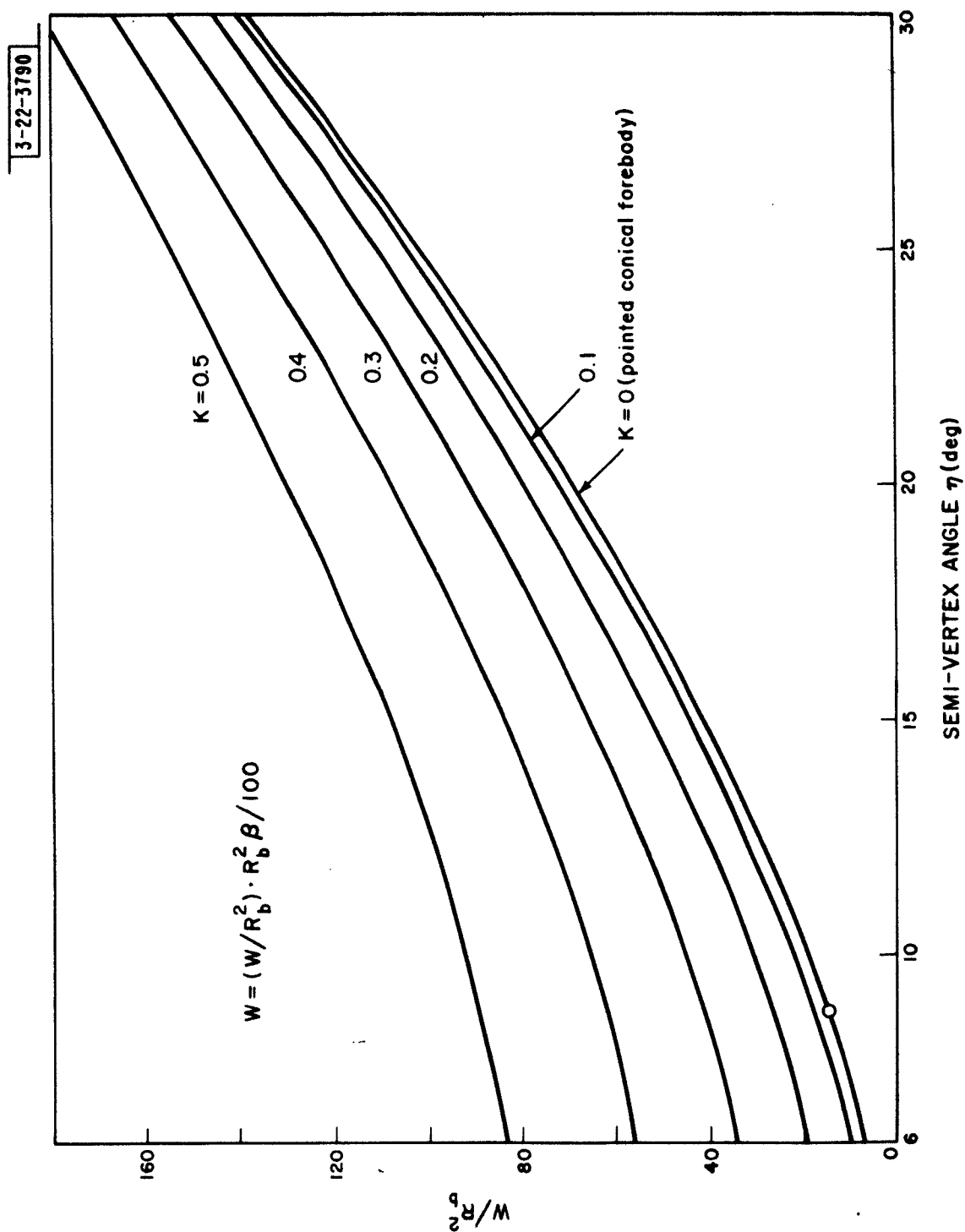


Fig. 3. Weights of blunted cone-spheres for ballistic coefficient  $\beta$ .

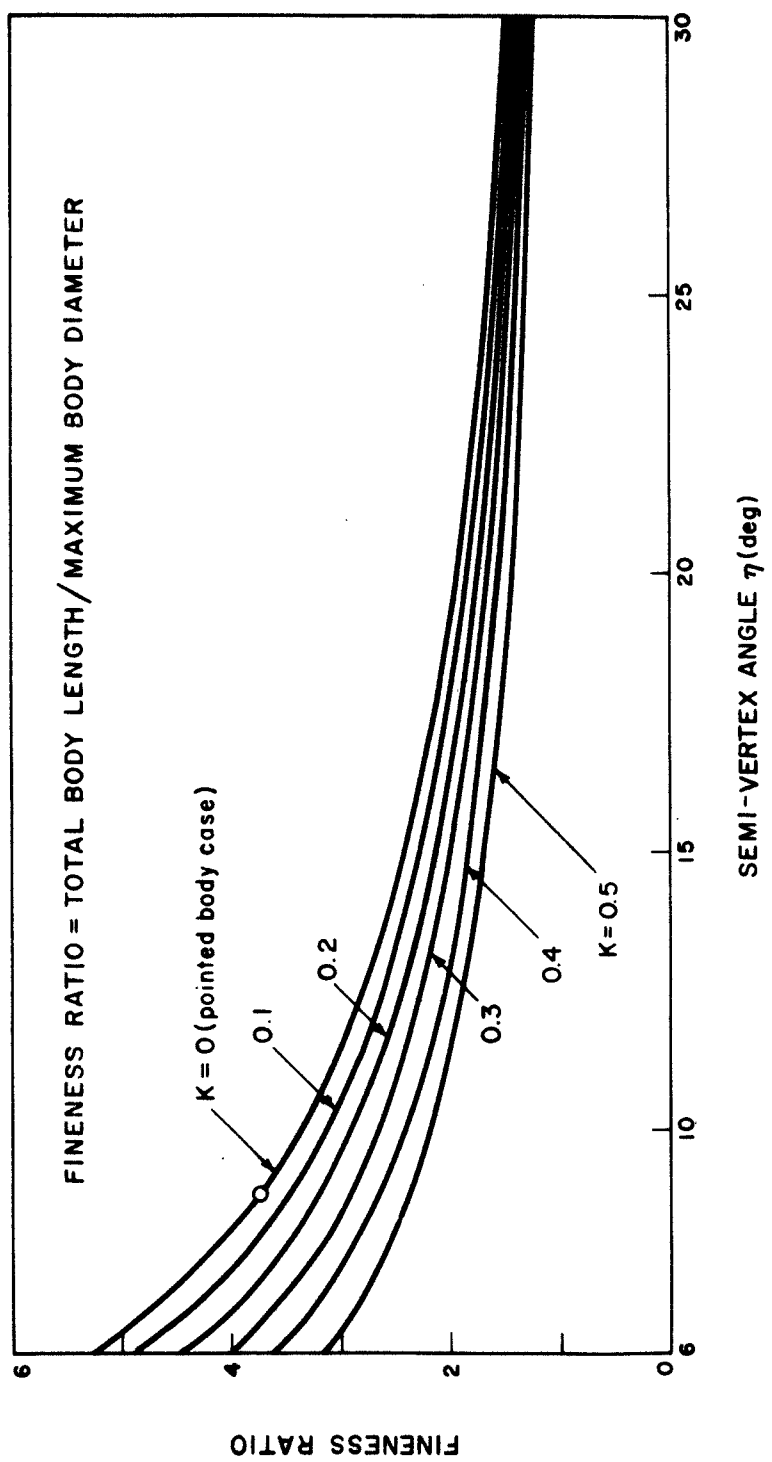


Fig. 4. Fineness ratios for blunted cone-spheres.

List of Symbols

$\alpha$	angle of attack (from body axis to relative-velocity vector)
$x, R, \omega$	cylindrical coordinates, $x$ along axis of symmetry
$R(x)$	body-radius in $(R, \omega)$ - plane
$R'(x)$	rate of change of body-radius along axis of symmetry
$x_{cg}$	body center of gravity (distance from nose)
$R_n, R_b$	nose-radius, base-radius of body
$\kappa$	"bluntness ratio", $\kappa = R_n/R_b$
$\ell$	total length exposed to flow, "wetted" length
$L$	total length of body
$F$	fineness ratio, $F = L/2R_b$
$\eta$	semi-vertex angle for conical midsection
$\theta$	local inclination of body surface, $\theta = \arctan R'(x)$
$q$	angular pitch-rate about transverse axis through $x_{cg}$
$p, C_p$	local pressure, local pressure coefficient
$p_\infty, \rho_\infty$	free-stream pressure, free-stream density
$v_\infty, M_\infty$	free-stream velocity, free stream Mach number
$q_\infty$	dynamic pressure, $q_\infty = \frac{1}{2} \rho_\infty v_\infty^2$
$v_n$	component of free-stream velocity normal to body surface
$A$	reference-area for non-dimensional coefficients
$C_X$	axial-force coefficient, $C_X = \text{axial force}/q_\infty A$
$C_D$	drag-force coefficient, $C_D = \text{drag force}/q_\infty A$

### References

1. Tobak, M. and Wehrend, W. R. : Stability Derivatives of Cones at Supersonic Speeds, NASA Technical Note 3788 (1956).
2. Ehret, D. M. : Accuracy of Approximate Methods for Predicting Pressures on Pointed Non-lifting Bodies of Revolution in Supersonic Flow, NASA Technical Note 2764 (1952).
3. Margolis, K. : Theoretical Evaluation of the Pressures, Forces and Moments at Hypersonic Speeds Acting on Arbitrary Bodies of Revolution Undergoing Separate and Combined Angle-of-Attack and Pitching Motions, NASA Technical Note D652 (1961).
4. Grimmer, G., Williams, E. P., and Young, G. B. W. : Lift on Inclined Bodies of Revolution in Hypersonic Flow, Journal of the Aeronautical Sciences, Vol. 17, No. 11 (November 1950), pp. 675 - 690.

Distribution ListDirector's Office

D. E. Dustin

Division 1

R. E. Rader

Division 2

C. R. Wieser

S. H. Dodd

Division 3

J. V. Harrington

Division 4

J. Freedman

J. W. Meyer

Division 7

D. D. Jacobus

Group 21

O. V. Fortier

P. J. Harris

Group 22

V. A. Nedzel

J. F. Nolan

W. I. Wells

A. Armenti

M. Athanassiades

T. Bartee

R. Bergemann

N. Brigham

Group 22 (cont'd.)

L. F. Cianciolo

D. F. Clapp

E. L. Eaton

P. L. Falb

A. Freed

L. A. Gardner

L. A. Globus

A. Grometstein

H. J. Hagler

J. H. Halberstein

R. C. Holland

J. M. Holst

C. Hopkins

L. Kleinrock

A. Knoll

E. Korngold

L. Krafft

H. J. Kushner

W. Z. Lemnios

D. L. Lovenvirth

A. D. MacGillivray

M. M. Marill

L. M. Meixsell

L. Murray

B. Nanni

C. E. Nielsen

R. C. Norris

J. H. Pannell

E. W. Pike

D. Reiner

J. Rheinstein

D. J. Sakrison

J. Salerno

B. J. Schafer

D. Schneider

M. Schneider

F. C. Schweppe

A. F. Smith

J. S. Strano

H. Sussman

Group 22 (cont'd.)

C. W. Uskavitch

J. L. Vernon

J. B. Williams

J. M. Winett

P. E. Wood

PA File - J. Lankgjen

Group 24

P. Youtz

Group 25

H. Sherman

R. Enticknap

M. S. Macrakis

Group 26

R. H. Kingston

F. L. McNamara

Group 28

J. A. Arnow

Group 32

P. B. Sebring

Group 312

G. F. Pippert

S. Edelberg

K. Kresa

Group 41

A. A. Galvin

J. B. Resnick

Distribution List (continued)

Group 42

W. W Ward  
P A Northrop  
C B Slade  
F Betts  
J B Cooper  
J B Jelatis  
B H Labitt  
V C Martins  
W R Renhult  
R G Sandholm  
A F Standing  
C M Steinmetz  
R C Yost

Group 43

J G Barry

Group 46

C W Jones

Group 47

D L Clark

Group 48

R C Eutman

Group 71

F G. DeSantis  
P Alberti

Group 744

J. F Hutzenlaub